

Oxidation Chemistry of Poly(ethylene glycol)-Supported Carbonylruthenium(II) and Dioxoruthenium(VI) *meso*-Tetrakis(pentafluorophenyl)porphyrin

Jun-Long Zhang, Jie-Sheng Huang, and Chi-Ming Che*^[a]

Abstract: [Ru^{II}(F₂₀-tpp)(CO)] (**1**, F₂₀-tpp = *meso*-tetrakis(pentafluorophenyl)porphyrinato dianion) was covalently attached to poly(ethylene glycol) (PEG) through the reaction of **1** with PEG and sodium hydride in DMF. The water-soluble PEG-supported ruthenium porphyrin (PEG-**1**) is an efficient catalyst for 2,6-Cl₂pyNO oxidation and PhI=NTs aziridination/amidation of hydrocarbons, and intramolecular amidation of sulfamate esters with PhI-

(OAc)₂. Oxidation of PEG-**1** by *m*-CPBA in CH₂Cl₂, dioxane, or water afforded a water-soluble PEG-supported dioxoruthenium(VI) porphyrin (PEG-**2**), which could react with hydrocarbons to give oxidation products in up to 80% yield. The behavior of the two

PEG-supported ruthenium porphyrin complexes in water was probed by NMR spectroscopy and dynamic light-scattering measurements. PEG-**2** is remarkably stable to water. The second-order rate constants (*k*₂) for the oxidation of styrene and ethylbenzene by PEG-**2** in dioxane–water increase with water content, and the *k*₂ values at a water content of 70% or 80% are up to 188 times that obtained in ClCH₂CH₂Cl.

Keywords: homogeneous catalysis • oxidation • porphyrinoids • ruthenium • supported catalysts

Introduction

The importance of metalloporphyrin-mediated hydrocarbon functionalization in organic catalysis^[1–4] is well documented, and oxygen^[1a–d,h,j]/nitrogen^[1e,f]/carbon^[1g–i]-atom transfer reactions catalyzed by metalloporphyrins have begun to emerge as useful reactions that have found applications in organic synthesis.^[1] An appealing approach to practical metalloporphyrin catalysts is to attach a metalloporphyrin to a polymer or mesoporous silica material;^[2–4] this method facilitates product separation and catalyst recovery/reuse. Interestingly, the heterogenization of a ruthenium porphyrin catalyst by covalent attachment to Merrifield's peptide resin was found to result in excellent reactivity, selectivity, and versatility in alkene epoxidation.^[2a] Homogeneous epoxidation and cyclopropanation of alkenes catalyzed by manganese^[4a]/iron^[4b]/ruthenium^[4c] porphyrin complexes covalently attached to

dendrimers have also demonstrated high reactivity and selectivity.

Metalloporphyrin-mediated hydrocarbon functionalization is important in biomimetic studies as well.^[1d,5–11] Notable examples include 1) regioselective oxidation of steroids by manganese porphyrin complexes that have β-cyclodextrins^[6a,b,d] or by manganese/iron porphyrin complexes with appending cholenic acid moieties in vesicle bilayer assemblies,^[7] 2) regioselective C=C bond cleavage of carotenoids by a ruthenium porphyrin complex containing β-cyclodextrins,^[8] and 3) progressive epoxidation of polybutadiene by a topologically linked manganese porphyrin.^[9] These catalytic systems mimic the activities of cytochrome P-450 enzymes, carotene dioxygenases, and toroidal enzymes (such as exo- and endonucleases), respectively.

It has been proposed that hydrocarbon oxidation reactions mediated by metalloporphyrins involve reactive oxometalloporphyrin intermediates.^[1a–d] Investigation on the reactivity of oxometalloporphyrins attached to macromolecules is important for understanding the mechanism of hydrocarbon oxidation catalyzed by polymer-supported metalloporphyrins or by related native enzymes (the metalloporphyrin active sites of which are attached to protein chains), and could provide useful information for design of both new catalysts and enzyme mimics. Up to now, a series of oxometalloporphyrins containing Fe^{IV}=O,^[12a–d] Cr^V=

[a] J.-L. Zhang, Dr. J.-S. Huang, Prof. C.-M. Che
Department of Chemistry and
Open Laboratory of Chemical Biology of the
Institute of Molecular Technology for Drug Discovery and Synthesis
The University of Hong Kong, Pokfulam Road, Hong Kong (China)
Fax: (+852) 2857-1586
E-mail: cmche@hku.hk

Supporting information for this article is available on the WWW
under <http://www.chemeurj.org/> or from the author.

O,^[12f] Mn^{IV/V}=O,^[12e,ij] and Ru^{VI}=O^[13] groups that are reactive toward hydrocarbon oxidation are known; an in situ generated Mn^{IV}=O porphyrin encapsulated into a polymer dendrigraft was reported recently,^[12j] but, to the best of our knowledge, covalent attachment of these oxometalloporphyrins to synthetic macromolecules remains unrealized.

We are interested in constructing a soluble macromolecule-supported oxometalloporphyrin by covalently linking a reactive hydrophobic dioxoruthenium(vi) porphyrin [Ru^{VI}(por)O₂]^[13] to hydrophilic poly(ethylene glycol) (PEG). This was prompted by the reports that [Ru^{VI}(por)O₂] are reactive toward hydrocarbon oxidation^[13] and could be isolated, and several soluble PEG-supported manganese^[4f,10]/ruthenium^[4d] porphyrins are active hydrocarbon oxidation catalysts. The amphiphilic PEG-supported dioxoruthenium(vi) porphyrin is expected to dissolve in water through, for example, micelle formation, providing a unique opportunity of developing hitherto rarely explored oxidation chemistry of oxometalloporphyrins in aqueous media.

In this work, we report the covalent attachment of oxidatively robust [Ru^{II}(F₂₀-tpp)(CO)] (**1**, F₂₀-tpp = *meso*-tetraakis(pentafluorophenyl)porphyrinato(2-))^[14] to PEG to form a polymer-supported ruthenium porphyrin (PEG-**1**) and the preparation of a PEG-supported dioxoruthenium(vi) porphyrin (PEG-**2**; Figure 1), by oxidation of PEG-**1** with *m*-chloroperoxybenzoic acid (*m*-CPBA), along with PEG-**1**-catalyzed oxidation/amidation of hydrocarbons. Kinetic studies on the oxidation of a series of hydrocarbons by PEG-**2** in organic solvents (such as ClCH₂CH₂Cl, benzene, and dioxane) and in aqueous solutions are described.

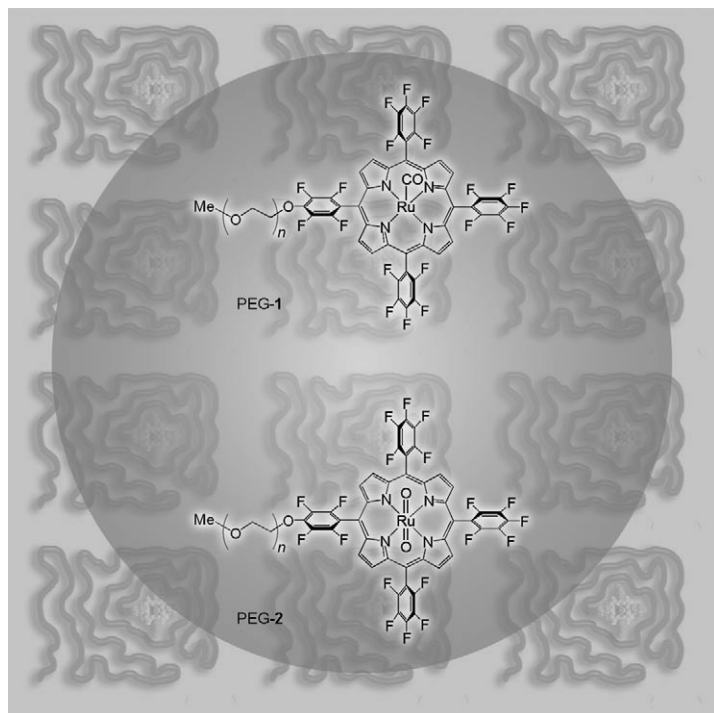


Figure 1. Schematic structure of PEG-**1** and PEG-**2**.

Results

Synthesis and characterization of PEG-supported ruthenium porphyrins PEG-1** and PEG-**2**:** The carbonylruthenium(II) porphyrin **1** has previously been reported to be an active and robust catalyst for oxidation of C–H bonds.^[14] This complex could be functionalized through substitution reaction of the *para*-F atom of the perfluorophenyl ring with nucleophilic reagents, such as primary/secondary amines and alkoxide ions.^[15] In the present work, PEG-**1** was obtained by treating excess **1** with a solution of sodium PEG salt generated in situ from sodium hydride and PEG in DMF. The progress of the reaction was followed by thin-layer chromatography (TLC). After purification, PEG-**1** was obtained in 70% yield based on the amount of PEG used. PEG-**2** was prepared by addition of *m*-CPBA to a solution of PEG-**1** in CH₂Cl₂. Both PEG-**1** and PEG-**2** are red hygroscopic solids, soluble in CH₂Cl₂, CHCl₃, ethanol, dioxane, and water, but insoluble in acetone and diethyl ether. A control experiment was performed by adding **1** (1 μmol, 1.1 mg) to a solution of PEG (0.1 mmol, 0.5 g) in water (100 mL); the ruthenium porphyrin complex was rapidly precipitated out, revealing that a physical mixture of **1** and PEG could not solubilize the former in water.

The ¹H NMR spectrum of PEG-**1** in CDCl₃ shows a broad signal at δ = 8.82 ppm which is assigned to the pyrrolic protons (β-H) of the porphyrin macrocycle; a similar β-H chemical shift (δ = 8.78 ppm) was found for **1**. In the case of PEG-**2**, the β-H signal appears as a broad peak at δ = 9.20 ppm, similar to the β-H chemical shift of [Ru^{II}(F₂₀-tpp)O₂] (**2**, δ = 9.18 ppm).

The ¹⁹F NMR spectrum of PEG-**1** in CDCl₃ at room temperature reveals three sets of signals at δ = –136.7 to –141.5, –151.9 to –152.6, and –157.0 to –163.0 ppm, which are assigned to the *ortho*-, *para*-, and *meta*-F atoms by comparison with the related ¹⁹F NMR signals of **1** (δ_F –136.1, –138.1 (*ortho*-F), –152.2 (*para*-F), –161.5, –162.2 ppm (*meta*-F)). PEG-**2** shows broad signals at δ = –135.6 to –139.0 (*ortho*-F), –150.4 (*para*-F), and –157.6 to –161.5 ppm (*meta*-F) in CDCl₃, while the related ¹⁹F signals of **2** are at δ = –136.8 (*ortho*-F), –149.2 (*para*-F), and –161.2 ppm (*meta*-F).

The IR spectrum of PEG-**1** shows an intense ν(CO) band at 1954 cm^{–1}; such a band is absent in the IR spectrum of PEG-**2**, the latter displays a weak band at 830 cm^{–1} assignable to the ν(RuO₂) stretch.^[13] The UV/Vis spectrum of PEG-**1** in CH₂Cl₂ features Soret band at 406 nm and β band at 526 nm, similar to those of **1**. For PEG-**2**, the absorption bands at 413 (Soret) and 508 nm (β) are similar to those of **2** at 412 and 506 nm, respectively. The slightly red-shifted Soret and β bands of PEG-**1** and PEG-**2** relative to those of **1** and **2**, respectively, could be due to the substitution of the *para*-F of a perfluorophenyl ring by the alkoxy group of the PEG chain.

For PEG-**1**, the integration ratio of the porphyrin β-H signal to the PEG methoxy signal gave a loading of **1** of 0.10 mmol g^{–1}. Based on the absorbance of the Soret band at

406 nm and assuming that the ϵ values of PEG-1 and **1** at 406 nm are the same (with 10% error), the loading of **1** in PEG-1 was also estimated to be 0.10 mmol g^{-1} . For PEG-2, the integration of the β -H and the PEG methoxy signals revealed that the loading of **2** was about 0.10 mmol g^{-1} , suggesting that no appreciable ruthenium porphyrin leaching occurred during oxidation of PEG-1 to PEG-2 by *m*-CPBA in CH_2Cl_2 .

Behavior of PEG-1 in aqueous solution

NMR studies: In NMR spectroscopy, signal broadening (which is often accompanied by change in relaxation time and decreased intensity, and reflects a change in microenvironment of the nuclei) has been taken as an indication for aggregation of amphiphilic polymers^[16] or restriction of internal nuclei mobility in water.^[17] We found that while the ^1H NMR spectrum of PEG-1 in CDCl_3 shows well-resolved signals of the PEG chain ($\delta=3.35\text{--}4.78 \text{ ppm}$) and the porphyrin ring β -H protons ($\delta=8.82 \text{ ppm}$), in D_2O the signal of the porphyrin ring β -H proton ($\delta=8.80 \text{ ppm}$) is markedly broadened (although the signals of the PEG chain are only slightly affected). The ^{19}F NMR spectrum of PEG-1 in D_2O is almost featureless, in contrast to the well-resolved signals in CDCl_3 .

To further investigate the solvent effect on the microenvironment of ruthenium porphyrin core supported by PEG chain, we measured the ^{19}F NMR spectra of PEG-1 in $[\text{D}_8]\text{dioxane-D}_2\text{O}$ with water content increasing from 0 to 100% at 10% or 20% intervals (Figure 2). Upon increasing

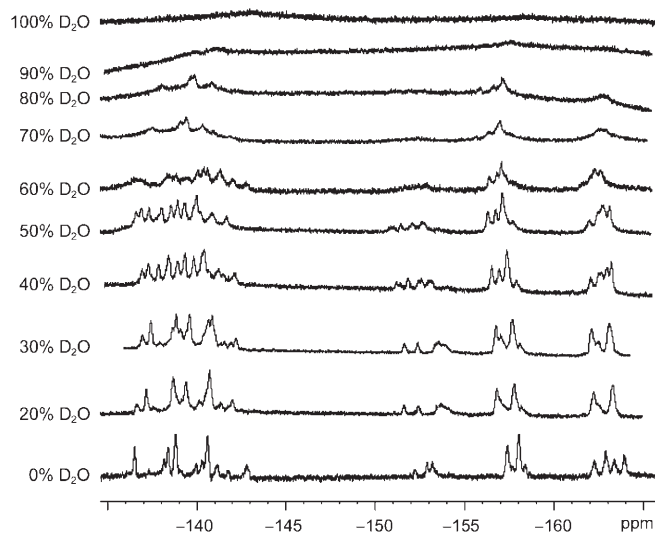


Figure 2. ^{19}F NMR spectra of PEG-1 ($2.4 \times 10^{-3} \text{ M}$) in $[\text{D}_8]\text{dioxane-D}_2\text{O}$ at different water contents (v/v).

the water content from 0 to 30%, the signals were broadened and slightly changed. As the water content increased to 40–60%, the signals were further broadened and became more complicated. At water contents of $\geq 70\%$, the signals were very broad or even hard to be observed.

Two-dimensional nuclear Overhauser effect NMR spectroscopy (NOESY) was employed to probe the interaction of PEG-1 with styrene (a substrate in the oxidation reactions described below) in a mixture of PEG-1 and styrene in CDCl_3 or D_2O (Figure 3). In CDCl_3 , the signals of styrene in

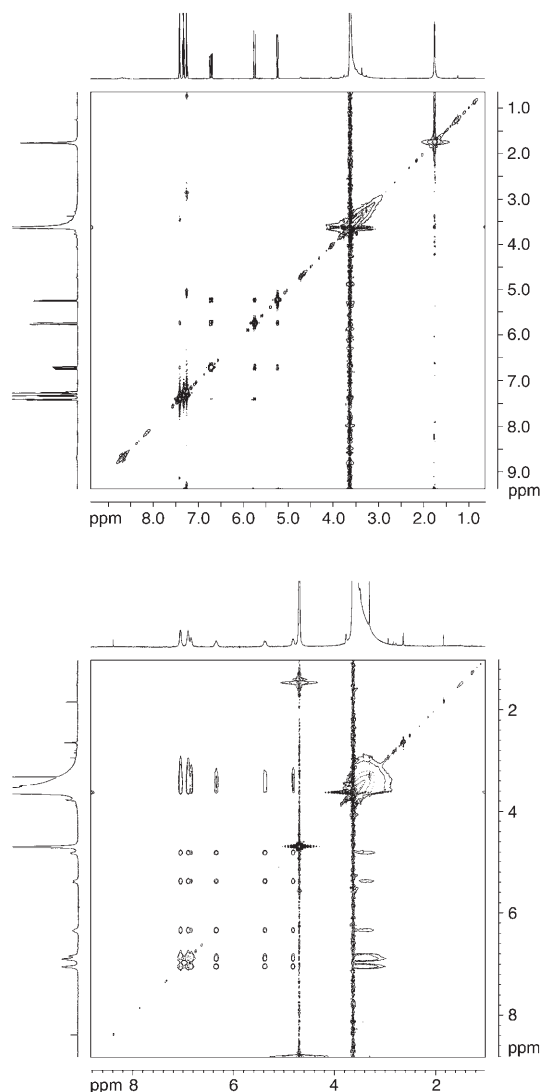


Figure 3. 2D ^1H NMR spectra (NOESY) of a mixture of PEG-1 ($1.2 \times 10^{-3} \text{ M}$) and styrene ($2.0 \times 10^{-3} \text{ M}$) in CDCl_3 (upper) and D_2O (lower).

the mixture are similar to those of free styrene and no NOE between styrene and the PEG-chain/porphyrin was observed. However, in D_2O , the spectrum of the mixture features broad, poorly resolved, and upfield shifted ($\Delta\delta \approx 0.30 \text{ ppm}$) signals of styrene and there is an NOE between the styrene and the PEG chain (but not between styrene and the porphyrin ring). A control experiment using a mixture of styrene and PEG in D_2O under the same conditions showed similar ^1H NMR chemical shifts to those of the PEG-1/styrene mixture, suggesting that styrene molecules were encapsulated by the PEG chains in water.

The effect of water content on the interaction between styrene and PEG-1 was examined by measuring the ^1H NMR spectra of a mixture of PEG-1 and styrene in $[\text{D}_8]$ dioxane- D_2O at different water contents; these experiments revealed a dependence of the chemical shift changes ($\Delta\delta$) of styrene on the water content as shown in Figure 4

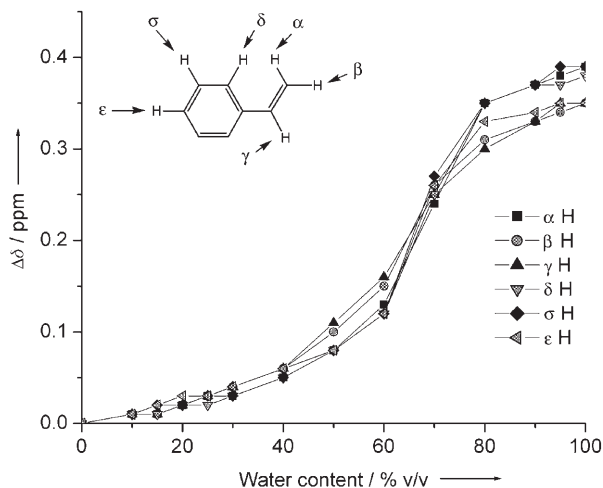


Figure 4. Change of ^1H NMR chemical shifts ($\Delta\delta$) of styrene protons as a function of water contents observed for a mixture of PEG-1 ($1.2 \times 10^{-3} \text{ M}$) and styrene ($2.0 \times 10^{-3} \text{ M}$) in $[\text{D}_8]$ dioxane- D_2O ($\Delta\delta = \Delta\delta_X^C - \Delta\delta_X^0$, in which $X = \alpha, \beta, \gamma, \delta, \sigma, \varepsilon$; $\Delta\delta_X = \delta_X - \delta_{\text{PEG}}$; δ_{PEG} is the chemical shift of the most intense signal of PEG; $\Delta\delta_X^C$ and $\Delta\delta_X^0$ are the values at water contents of C% and 0%, respectively).

(see also Table S1 in Supporting Information). Evidently, for all the styrene protons, the $\Delta\delta$ values increase with increasing water content in a similar manner, suggesting an “isotropic” effect of water content on the styrene proton resonances. The most dramatic increase of $\Delta\delta$ occurs at water contents of 60–80%.

Dynamic light-scattering studies: We measured the size of the particles in a solution of PEG-1 in water by dynamic light scattering. The average hydrodynamic diameter of the particles was observed to be about 34 nm. Reducing the solvent polarity by addition of dioxane led to increase in the size of the particles. The dependence of particle size on water content for the dioxane–water solution of PEG-1 is depicted in Figure 5 (see also Table S2 in Supporting Information).

Oxidation to PEG-2: Previous studies showed that dioxoruthenium(vi) porphyrins $[\text{Ru}^{\text{VI}}(\text{por})\text{O}_2]$ could be obtained by oxidation of $[\text{Ru}^{\text{II}}(\text{por})(\text{CO})]$ with *m*-CPBA or PhIO in CH_2Cl_2 and alcohol.^[13] However, there has been no report on the generation of dioxoruthenium(vi) porphyrin in aqueous medium. In this work, we examined the reaction of PEG-1 with H_2O_2 , TBHP (*tert*-butyl hydroperoxide), 2,6- Cl_2pyNO (2,6-dichloropyridine *N*-oxide), PhIO, or *m*-CPBA in aqueous solutions at room temperature by UV/Vis spectroscopy.

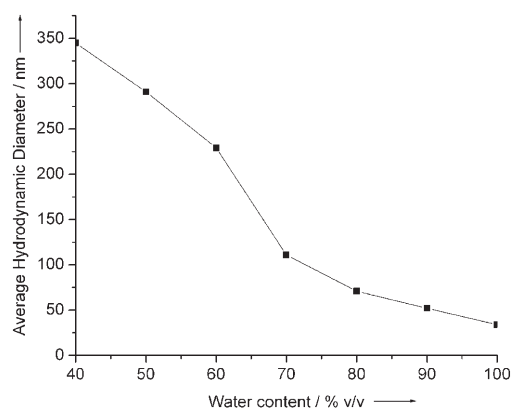


Figure 5. Average particle sizes of PEG-1 in dioxane–water solution at different water contents.

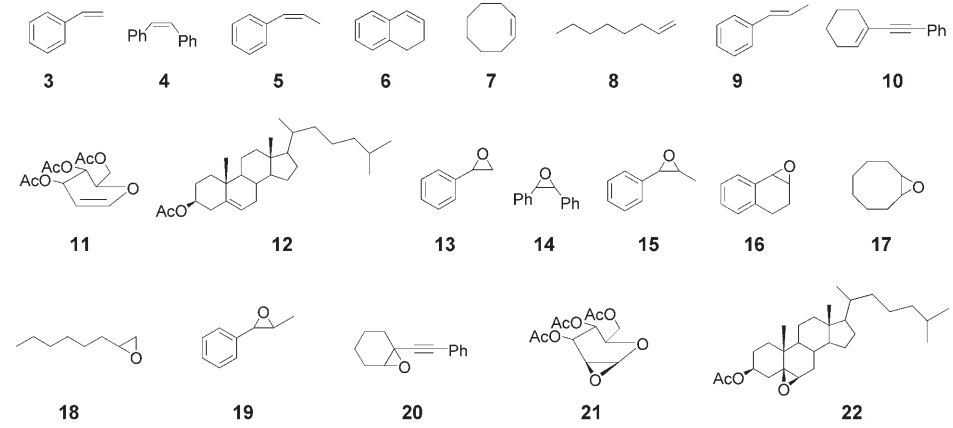
As listed in Table S3 (see Supporting Information), *m*-CPBA, PhIO, and TBHP could oxidize PEG-1 and **1** to PEG-2 and **2**, respectively, in CH_2Cl_2 . The oxidation by TBHP was much slower (2 h, entry 10) than by *m*-CPBA and PhIO (several minutes, entries 1 and 4). *m*-CPBA was found to be a suitable oxidant for generation of PEG-2 from PEG-1 in water (entry 2) and in dioxane–water (50% v/v) (entry 3). Conversion of PEG-1 to PEG-2 in dioxane–water (50% v/v) could also be effected by using PhIO and TBHP, but a 2 h reaction time was needed (entries 6 and 12). In water, neither PhIO nor TBHP was observed to oxidize PEG-1 to PEG-2 (entries 5 and 11). Complex **1** is insoluble in water and no reaction was found with the above oxidants in this solvent (entries 5, 8, 11, and 14). Even in the mixed solvent dioxane–water (50% v/v), PhIO and *m*-CPBA could not oxidize **1** to **2** (the reaction shifted the Soret band to 398 nm and the β band to 540 nm, which are substantially different from those of **2**) (entries 3 and 6). 2,6- Cl_2pyNO was not an effective oxidant for conversion of PEG-1 and **1** to PEG-2 and **2**, respectively (entries 7–9). In the case of H_2O_2 , its reaction with **1** and PEG-1 showed similar spectral changes in CH_2Cl_2 and dioxane–water: the Soret band blue shifted to 406 nm, the β band red shifted to 560 nm, and a new band at 600 nm developed; such spectral features do not correspond to the formation of **2** (entries 13 and 15). In water, no reaction was observed between PEG-1 and H_2O_2 at room temperature even at a reaction time of 4 h.

^1H NMR spectroscopy was used to monitor the reaction between PEG-1 (1 mM) and *m*-CPBA (10 equiv) in D_2O . This reaction was found to shift the β -H signal of the porphyrin ring at $\delta = 8.82$ ppm to $\delta = 9.20$ ppm within 5 minutes, indicating the formation of PEG-2.

Catalytic properties of PEG-1

Oxygen-atom transfer reactions: In a previous report, we demonstrated the activity of PEG-supported ruthenium porphyrin catalysts in epoxidation of alkenes with 2,6-

Table 1. Epoxidation of alkenes (**3–12**) with 2,6-Cl₂pyNO catalyzed by PEG-**1**.^[a]



| Entry | Substrate | Product | <i>t</i> [h] | Conv. [%] ^[b] | Yield [%] (TON) ^[c] | Config. ^[d] |
|-------|-----------|-----------|--------------|--------------------------|--------------------------------|------------------------|
| 1 | 3 | 13 | 24 | 82 | 76 (620) | n.d. ^[e] |
| 2 | 4 | 14 | 24 | 86 | 88 (750) | <i>cis</i> |
| 3 | 5 | 15 | 24 | 88 | 82 (720) | <i>cis</i> |
| 4 | 6 | 16 | 24 | 90 | 92 (820) | n.d. |
| 5 | 7 | 17 | 24 | 90 | 99 (880) | n.d. |
| 6 | 8 | 18 | 24 | 82 | 99 (820) | n.d. |
| 7 | 9 | 19 | 24 | 72 | 88 (630) | <i>trans</i> |
| 8 | 10 | 20 | 24 | 82 | 99 (810) | n.d. |
| 9 | 11 | 21 | 24 | 68 | 99 (670) | $\alpha:\beta=9:1$ |
| 10 | 12 | 22 | 24 | 95 | 99 (940) | β |

[a] All reactions were carried out in CH₂Cl₂ at 50 °C in a sealed flask (unless otherwise noted) with catalyst/2,6-Cl₂pyNO/alkene molar ratio of 1:1100:1000. [b] Determined by GC or ¹H NMR spectroscopy by using internal standard method (1,4-dichlorobenzene or 1,3,5-tribromobenzene). [c] Based on the amount of consumed alkenes. TON=turnover number. [d] Determined by comparison with the ¹H NMR data or GC spectra of standard products. [e] n.d.=not determined.

Cl₂pyNO.^[4d] In this work, PEG-**1** was found to be a more reactive and robust oxidation catalyst.

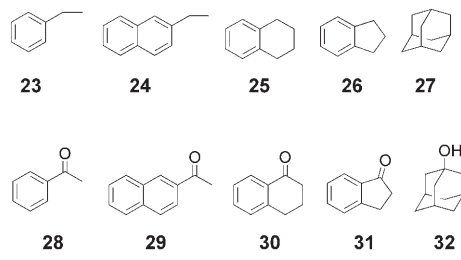
As depicted in Table 1, PEG-**1** is an efficient catalyst for epoxidation of a wide variety of alkenes with 2,6-Cl₂pyNO. In the cases of styrene, *cis*-stilbene, *cis*- β -methylstyrene, 1,2-dihydronaphthalene, cyclooctene, and 1-octene (substrates **3–8**, entries 1–6), the yields and selectivity of the epoxides (**13–18**) are comparable to those obtained with the reported PEG-, MCM-41-, and Merrifield's resin-supported ruthenium porphyrin catalysts.^[2a,3c,f,4d] For reactions with *trans*- β -methylstyrene (**9**), the *trans*-epoxide **19** was obtained in high yield (88 %, entry 7). The applicability of the “PEG-**1** + 2,6-Cl₂pyNO” protocol in the synthesis of organic building blocks has been examined. By using 1-phenethynyl cyclohexene (**10**) as substrate, the reaction afforded the corresponding epoxide **20**, which could be used for the synthesis of bioactive enediyne antitumor agents,^[18] in high yield (99 %, entry 8). 3,4,6-Tri-*O*-acetyl-D-glycal (**11**) was converted to the epoxide derivative **21**^[19] in 99 % yield with $\alpha:\beta$ ratio of 9:1. This α -selectivity is comparable to that obtained for [Ru^{II}(2,6-Cl₂tpp)(CO)] (2,6-Cl₂tpp = *meso*-tetrakis(2,6-dichlorophenyl)porphyrinato(2-)),^[3c] dendritic ruthenium porphyrins,^[4e] and for the ruthenium porphyrins immobilized on MCM-41^[3c] and Merrifield's peptide resin.^[2a] Cholesteryl acetate **12** was epoxidized to **22** in 99 % yield with complete β -selectivity, similar to the previously reported epoxidation using the “[Ru^{VI}(tmp)O₂] + air” (tmp = *meso*-tetramesityl-

porphyrinato(2-)) and “dendritic ruthenium porphyrin + 2,6-Cl₂pyNO” protocols.^[4c]

Groves and co-workers reported that **1** is an efficient and robust catalyst for 2,6-Cl₂pyNO oxidation of saturated C–H bonds.^[14] To test the catalytic activity of PEG-**1** toward C–H bond oxidation, we examined oxidation of ethylbenzene (**23**) with the “PEG-**1** + 2,6-Cl₂pyNO” protocol in CH₂Cl₂. At 40 °C for 24 h, acetophenone (**28**) was obtained in 99 % yield and the conversion of ethylbenzene was 52 % (entry 1, Table 2), which is lower than the conversion of 70 % obtained for catalyst **1** (entry 2, Table 2), but considerably higher than the conversion of 22 % obtained by using a previously reported PEG-supported ruthenium porphyrin catalyst.^[4d] Severin and Nestler reported that a cross-linked polymer-supported ruthenium porphyrin could catalyze oxidation of **23** to **28** in a high conversion of

74 %.^[2b] For the substrates ethylnaphthalene, 1,2,3,4-tetrahydronaphthalene, indane, and adamantane (**24–27**), the conversions obtained for PEG-**1** (entries 3–6, Table 2) are com-

Table 2. Oxidation of hydrocarbons (**23–27**) with 2,6-Cl₂pyNO catalyzed by PEG-**1**.^[a]



| Entry | Catalyst | Substrate | Product | <i>t</i> [h] | Conv. [%] ^[b] | Yield [%] (TON) ^[c] |
|-------|---------------|-----------|-----------|--------------|--------------------------|--------------------------------|
| 1 | PEG- 1 | 23 | 28 | 24 | 52 | 99 (50) |
| 2 | 1 | 23 | 28 | 24 | 70 | 99 (70) |
| 3 | PEG- 1 | 24 | 29 | 24 | 46 | 99 (40) |
| 4 | PEG- 1 | 25 | 30 | 24 | 60 | 99 (60) |
| 5 | PEG- 1 | 26 | 31 | 24 | 70 | 99 (70) |
| 6 | PEG- 1 | 27 | 32 | 24 | 65 | 80 (50) |

[a] All reactions were carried out in CH₂Cl₂ at 65 °C in a sealed flask, with catalyst/2,6-Cl₂pyNO/substrate molar ratio of 1:220:100 for entries 1–5 and 1:110:100 for entry 6. [b] Determined by GC or ¹H NMR spectroscopy by using internal standard method (1,4-dichlorobenzene or 1,3,5-tribromobenzene). [c] Based on the amount of consumed substrates. TON=turnover number.

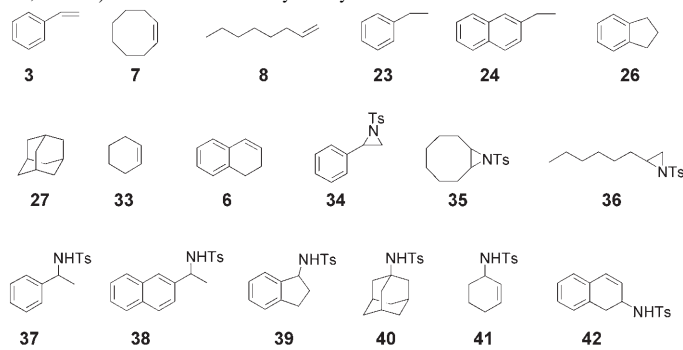
parable to those obtained for **1**. No reaction was found with benzene and naphthalene.

We also examined the epoxidation of styrene (0.1 mmol) with 2,6-Cl₂pyNO (0.15 mmol) in water (5 mL) by using catalyst PEG-1 (0.01 mmol). The reaction was conducted at room temperature for 24 h, affording benzaldehyde as main product with a styrene conversion of 5%. When PhIO was used as oxidant, no conversion of styrene was observed.

Nitrogen-atom-transfer reactions: Metal-mediated nitrogen-atom transfer to hydrocarbons is an appealing route to aziridines and amides.^[1e,f] Both ruthenium^[20] and manganese porphyrins^[21] were reported to be efficient catalysts for these reactions. However, there are few studies on supported metal catalysts for C–N bond formation reactions. Recently, we reported that the PEG-supported carbonylruthenium(II) porphyrin bearing *para*-chloro substituents on the porphyrin *meso*-phenyl groups exhibited moderate reactivity in catalyzing aziridination of alkenes.^[4d] We envisioned that replacing this carbonylruthenium(II) porphyrin core by **1** would lead to an efficient and robust PEG-supported ruthenium porphyrin catalyst for aziridination/amidation reactions.

Reactions of alkenes **3**, **7**, and **8** with PhI=NTs in CH₂Cl₂ at 40 °C for 4 h in the presence of a catalytic amount of PEG-1 at a catalyst/PhI=NTs/substrate molar ratio of 1:150:75 afforded aziridines **34–36** in 70–86% yields with 38–82% substrate conversions (entries 1–3, Table 3). Under similar conditions, PEG-1 catalyzed the PhI=NTs amidation

Table 3. Aziridination or amidation of hydrocarbons (**3**, **6–8**, **23–24**, **26–27**, and **33**) with PhI=NTs catalyzed by PEG-1.^[a]



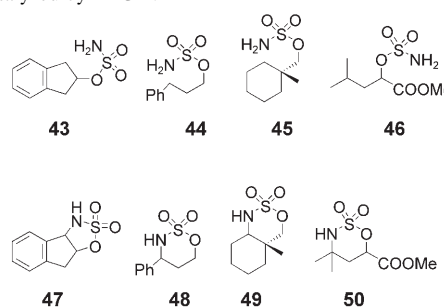
| Entry | Substrate | Product | <i>t</i> [h] | Conv. [%] ^[b] | Yield [%] ^[c] |
|------------------|-----------|-----------|--------------|--------------------------|--------------------------|
| 1 | 3 | 34 | 4 | 82 | 86 |
| 2 | 7 | 35 | 4 | 40 | 70 |
| 3 | 8 | 36 | 4 | 38 | 80 |
| 4 | 23 | 37 | 4 | 20 | 82 |
| 5 | 24 | 38 | 4 | 21 | 84 |
| 6 | 26 | 39 | 4 | 92 | 80 |
| 7 ^[d] | 26 | 39 | 8 | 36 | 73 |
| 8 | 27 | 40 | 4 | 90 | 80 |
| 9 | 33 | 41 | 4 | 45 | 90 |
| 10 | 6 | 42 | 4 | 94 | 80 |

[a] All reactions were carried out in CH₂Cl₂ at 40 °C with a catalyst/PhI=NTs/substrate molar ratio of 1:150:75 (unless otherwise noted). [b] Determined by GC by using internal standard method (1,4-dichloro- or 1,3,5-tribromobenzene). [c] Based on the amount of consumed substrate. [d] Catalyst/PhI=NTs/substrate molar ratio = 1:2000:1000.

of a series of benzylic hydrocarbons **6**, **23**, **24**, **26**, **27**, and **33** to give *N*-tosylamides **37–42** in 80–90% yields with 20–94% conversions (entries 4–6 and 8–10, Table 3). These results are comparable to those obtained for catalyst **1**^[20b,d] and better than those obtained for previously reported PEG-supported ruthenium porphyrin catalysts.^[4d] Under a low catalyst loading of 0.1 mol% (**1**/PhI=NTs/**26** molar ratio = 1:2000:1000), the PEG-1-catalyzed amidation of **26** afforded **39** in 73% yield with 36% substrate conversion (entry 7, Table 3), corresponding to a turnover number of 190.

In the presence of catalyst PEG-1 and Al₂O₃ with a catalyst/PhI(OAc)₂/substrate/Al₂O₃ molar ratio of 1:150:75:180, the reaction of sulfamate esters **43–46** with PhI(OAc)₂ in CH₂Cl₂ at 40 °C for 6 h afforded cyclic sulfamidates **47–50** in 86–90% yields (entries 1–4, Table 4) with retention of con-

Table 4. Intramolecular amidation of sulfamate esters (**43–46**) with PhI(OAc)₂ catalyzed by PEG-1.^[a]



| Entry | Substrate | Product | <i>t</i> [h] | Conv. [%] ^[b] | Yield [%] ^[c] |
|-------|-----------|-----------|--------------|--------------------------|--------------------------|
| 1 | 43 | 47 | 6 | 60 | 90 |
| 2 | 44 | 48 | 6 | 62 | 86 |
| 3 | 45 | 49 | 6 | 72 | 90 |
| 4 | 46 | 50 | 6 | 80 | 88 |

[a] All reactions were carried out in CH₂Cl₂ at 40 °C at a catalyst/PhI(OAc)₂/substrate/Al₂O₃ molar ratio of 1:150:75:180. [b] Determined by ¹H NMR spectroscopy by using the reaction mixture. [c] Based on the amount of consumed substrate.

figuration. The regioselectivity of these PEG-1-catalyzed intramolecular amidation reactions is similar to that for catalyst **1**^[20c] and dirhodium catalysts.^[22] Prior to this work, no polymer-supported catalyst has been reported to be efficient catalyst for intramolecular amidation of sulfamate esters.

Oxidation chemistry of PEG-2

Stability of PEG-2: We found that PEG-2 is rather stable in CH₂Cl₂ and dioxane. When these solutions were left standing for 4 h, less than 5% of PEG-2 was decomposed as revealed by UV/Vis spectroscopy. In dioxane–water, containing pyrazole (< 2% w/w, relative to the amount of dioxane) and with a water content of ≥ 40% (v/v), PEG-2 also displayed a remarkably high stability, as shown by the < 5% decrease in the absorbance at 414 nm over 2 h. This contrasts with the shift of the Soret (412 nm) and β (506 nm) bands of **2** to 396 and 545 nm, respectively, within 2 min under the same conditions (suggesting the formation of a μ-

oxo ruthenium porphyrin dimer). A control experiment showed that, for a physical mixture of **2** and two equivalents of PEG in dioxane containing 20% (v/v) water and 2% (w/w) pyrazole, **2** was rapidly converted to the μ -oxo ruthenium porphyrin dimer (as revealed by UV/Vis spectroscopy). These observations indicate that covalent attachment of **2** to the hydrophilic PEG chain dramatically enhances its stability toward water.

The effect of pH on the stability of PEG-**2** in water was examined by UV/Vis spectroscopy. When the pH was varied from 5 to 9, the Soret band absorbance of PEG-**2** decreased by <5% within 2 h. At pH >9 or <5, significant decomposition of PEG-**2** was observed, with the Soret band blue shifted to 402 nm and the β band red shifted to 520 nm upon standing for 2 h.

Stoichiometric oxidation of hydrocarbons by PEG-2: Treatment of styrene (1 mmol) with PEG-**2** (30 μ mol) in CH_2Cl_2 (5 mL) containing pyrazole (2% w/w) at room temperature for 2 h afforded styrene oxide in 70% yield, together with benzaldehyde in 10% yield (entry 1, Table 5). *cis*- β -Methyl-

conversion of $[\text{Ru}^{\text{IV}}(\text{por})\text{O}_2]$ to $[\text{Ru}^{\text{IV}}(\text{por})(\text{pz})_2]$ (Hpz = pyrazole).^[13c,f] In the absence of pyrazole, the kinetic profile for the Ru^{VI} to Ru^{IV} transformation was influenced by secondary reactions (possibly by the formation of Ru^{II} porphyrin) and deviated from first-order exponential decay. A similar phenomenon was observed for the oxidation of styrene by **2** or PEG-**2** in $\text{ClCH}_2\text{CH}_2\text{Cl}$; in these cases the conversion of the Ru^{VI} to Ru^{IV} species in the presence of pyrazole (2% w/w) is manifested by the decay of the Soret band at ~ 412 nm with concomitant development of a new absorption band at 402 nm.

We conducted kinetic studies on the oxidation of hydrocarbons by PEG-**2** or **2** in $\text{ClCH}_2\text{CH}_2\text{Cl}$ containing pyrazole (2% w/w) under the condition that $[\text{Ru}] \ll [\text{substrate}] < 1$ M. For all the substrates employed, the reactions exhibited pseudo-first-order kinetics and isosbestic spectral changes over four half-lives. The pseudo-first-order rate constants (k_{obs}) were determined by monitoring the disappearance of the Soret band ($\lambda_{\text{max}} = 414$ nm for PEG-**2** and 412 nm for **2**) of the dioxoruthenium(vi) porphyrins; the second-order rate constants (k_2) were determined from the plots of k_{obs} versus

[hydrocarbon] (Table 6). The k_2 values were unaffected by the pyrazole loading at 2–10% (w/w), and no appreciable reaction of PEG-**2** or **2** with pyrazole was observed within the timescale of the kinetic studies. For the reaction of styrene with PEG-**2**, the k_2 values in different solvents have been determined and are listed in Table S4 (see Supporting Information).

Table 5. Stoichiometric oxidation of hydrocarbons by PEG-**2** and **2** in CH_2Cl_2 , water, or dioxane–water.^[a]

| Entry | Substrate | Product | Solvent | Yield[%] ^[b] | |
|-------|-----------|--------------|------------------------------|------------------------------------|------------------------------------|
| | | | | PEG- 2 | 2 |
| 1 | 3 | 13 | CH_2Cl_2 | 70 | 74 |
| 2 | 3 | 51 | dioxane–water ^[c] | 70 | – |
| 3 | 5 | 15 | CH_2Cl_2 | 80 | 86 |
| 4 | 9 | 19 | CH_2Cl_2 | 62 | 66 |
| 5 | 23 | 28+52 | CH_2Cl_2 | 18 (28), 32 (52) | 22 (28), 36 (52) |
| 6 | 23 | 28 | dioxane–water ^[c] | 22 | – |

[a] All reactions were performed in the presence of pyrazole (2% w/w) at room temperature. [b] Based on the amount of PEG-**2**. [c] Water content: 40–90% v/v.

styrene, *trans*- β -methylstyrene, and ethylbenzene were also reactive with PEG-**2** under similar conditions, giving epoxides (**15** and **19**), ketone (**28**), or alcohol (**52**) in up to 80% yield (entries 3–5, Table 5). The oxidation of *cis*- β -methylstyrene gave a mixture of *cis*- and *trans*- β -methylstyrene oxides in a 10:1 ratio.

In dioxane–water (5 mL), containing pyrazole (2% w/w), and with a water content ranging from 40% to 90% v/v, the reaction of PEG-**2** (50 μ mol) with styrene (1 mmol) at room temperature for 2 h afforded benzaldehyde (**51**) in about 70% yield (entry 2, Table 5); oxidation of ethylbenzene by PEG-**2** under similar conditions gave acetophenone in about 22% yield (entry 6, Table 5).

Kinetic studies on the reactions of PEG-2 with hydrocarbons in $\text{ClCH}_2\text{CH}_2\text{Cl}$: Previous work demonstrated that oxidation of hydrocarbons by $[\text{Ru}^{\text{VI}}(\text{por})\text{O}_2]$ in organic solvents (such as $\text{ClCH}_2\text{CH}_2\text{Cl}$) containing pyrazole (2% w/w) features isosbestic UV/Vis spectral changes corresponding to a smooth

Kinetic studies on the reactions of PEG-2 with hydrocarbons in aqueous solution: UV/Vis spec-

Table 6. Second-order rate constants (k_2) for oxidation of hydrocarbons by PEG-**2** and **2** in $\text{ClCH}_2\text{CH}_2\text{Cl}$ containing pyrazole (2% w/w) at 298 K.^[a]

| Entry | Substrate | $k_2 \times 10^3$ [$\text{dm}^3 \text{mol}^{-1} \text{s}^{-1}$] | |
|-------|---------------------------------------|---|-----------------|
| | | PEG- 2 | 2 |
| 1 | styrene | 7.7 ± 0.3 | 14.0 ± 0.2 |
| 2 | 4-fluorostyrene | 9.0 ± 0.3 | 14.9 ± 0.8 |
| 3 | 4-chlorostyrene | 11.5 ± 0.4 | 16.8 ± 0.3 |
| 4 | 4-methylstyrene | 17.8 ± 0.7 | 24.2 ± 1.0 |
| 5 | 4-methoxystyrene | 37.4 ± 1.2 | 60.4 ± 1.5 |
| 6 | <i>cis</i> - β -methylstyrene | 8.6 ± 0.3 | 9.7 ± 0.5 |
| 7 | <i>trans</i> - β -methylstyrene | 11.4 ± 0.2 | 14.0 ± 0.6 |
| 8 | cyclohexene | 32.8 ± 1.1 | 41.2 ± 1.3 |
| 9 | <i>cis</i> -stilbene | 3.8 ± 0.2 | 4.3 ± 0.3 |
| 10 | <i>trans</i> -stilbene | 12.9 ± 0.3 | 20.1 ± 1.2 |
| 11 | cyclooctene | 9.5 ± 0.3 | 12.4 ± 1.3 |
| 12 | ethylbenzene | 0.81 ± 0.03 | 1.01 ± 0.06 |
| 13 | cumene | 0.48 ± 0.02 | 0.56 ± 0.03 |

[a] Pyrazole was not found to interfere with the rate-limiting step of the hydrocarbon oxidation reactions.

tral changes for the oxidation of styrene or ethylbenzene by PEG-2 in dioxane containing 40% (v/v) water and 2% (w/w) pyrazole showed an isosbestic transformation due to conversion of Ru^{VI} to Ru^{IV} species (we chose dioxane as an organic media because this solvent could dissolve the substrates and is less prone to substrate diffusional limitation). Similar spectral features were also observed for the same reaction in dioxane–water mixtures with different water contents (40–90%; see, for example, Figure 6). The oxidation of

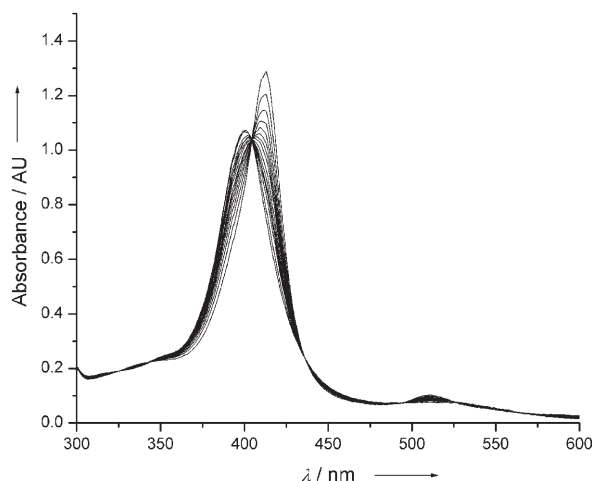


Figure 6. UV/Vis spectral changes during reaction of PEG-2 with styrene (0.0036 M) in dioxane–water (70% water, v/v) containing pyrazole (2% w/w) at 298 K (time scan: 3000 s, interval: 45 s). The isosbestic points were located at 402 and 436 nm.

styrene or ethylbenzene by PEG-2 in dioxane–water exhibited pseudo-first-order kinetics under the condition [substrate] \gg [PEG-2], like that in ClCH₂CH₂Cl. The pseudo-first-order rate constants (k_{obs}) at different substrate concentrations and water contents were determined by monitoring the disappearance of the Soret band of PEG-2 at $\lambda_{\text{max}} = 414$ nm. As styrene or ethylbenzene is virtually insoluble in water, increasing water content in dioxane–water would impose limitation on the substrate concentration that could be used in kinetic studies. Table 7 lists the k_2 values for the oxidation of styrene or ethylbenzene by PEG-2 in dioxane–water at different water contents.

Table 7. Second-order rate constants (k_2) for oxidation of styrene and ethylbenzene by PEG-2 in dioxane–water with different water contents at 298 K.^[a]

| Entry | Water content [% v/v] | $k_2 \times 10^3$ [dm ³ mol ⁻¹ s ⁻¹] | |
|-------|-----------------------|--|--------------|
| | | styrene | ethylbenzene |
| 1 | 40 | 34.8 ± 1.6 | 2.9 ± 0.2 |
| 2 | 50 | 54.4 ± 3.3 | 7.2 ± 0.2 |
| 3 | 60 | 89.0 ± 2.0 | 15.5 ± 0.9 |
| 4 | 65 | 304.8 ± 8.9 | 39.9 ± 3.1 |
| 5 | 70 | 479.0 ± 39.5 | 99.5 ± 5.4 |
| 6 | 80 | 548.0 ± 37.3 | 152.0 ± 9.7 |
| 7 | 90 | 570.9 ± 28.1 | 161.3 ± 14.7 |

[a] All reactions were performed in the presence of pyrazole (2% w/w) (pyrazole was not found to interfere with the rate-limiting step of the hydrocarbon oxidation reactions).

Discussion

PEG has commonly been used as a support or non-ionic surfactant in organic catalysis, combinatorial chemistry, and biological studies for its good solubility in many solvents (including water), easy recovery by simple precipitation or membrane separation, and biological compatibility.^[23] In catalysis, PEG-supported metal catalysts were found to exhibit comparable reactivity and selectivity to the unsupported counterparts and could be reused several times with slight decrease in product yield and selectivity.^[4d,f] PEG is a water-soluble polymer containing hydrophobic moieties; in aqueous solution, the hydrophobic moieties could bind (or interact with) nonpolar substrates to form a stable supramolecule. For the reactions involving nonpolar substrates and PEG in aqueous solution, hydrophobic effect^[24] might be important. To probe the formation of hydrophobic microdomains from aggregation of the hydrophobic moieties (to minimize their exposure to water) and the biomimetic behavior of PEG-based polymer systems in aqueous solutions, a variety of NMR techniques including relaxation time^[25a]/chemical shift^[25b] measurements and pulse gradient spin-echo (PGSE) NMR^[25c] were employed. Some fluorescent probes sensitive to the surrounding microenvironment have been used to study micellization of PEG polymers in water.^[26]

The reactivity, stability, and selectivity of metal catalysts or artificial enzymes and the corresponding reactive oxo intermediates in aqueous solution could be significantly different from that in organic solvents. So far few reactive oxometalporphyrin intermediates are stable enough for isolation. The isolable, reactive dioxoruthenium(vi) porphyrins previously reported in the literature^[13] are insoluble in water; it is not feasible to study their oxidation chemistry in aqueous solution. In this regard, the water solubility and stability of the PEG-supported dioxoruthenium(vi) porphyrin PEG-2, would be of interest.

Effect of solvent on configurations of PEG-1 and PEG-2:

The well-resolved ¹H NMR signals of the PEG chain of PEG-1 in CDCl₃ and D₂O indicate that the PEG moiety is well solvated in both solvents. The marked broadening of the porphyrin ring β-H signal of PEG-1 by changing solvent from CDCl₃ to D₂O and the almost featureless ¹⁹F NMR spectrum of PEG-1 in D₂O suggest a poor solvation of the porphyrin core in water. This can be rationalized by the formation of micellar assemblies in a solution of PEG-1 in water, with the hydrophobic porphyrin cores embedded in the interior of the micelles, which restricts the motion of porphyrin H and F nuclei and shortens their relaxation times. Similar micellar assemblies could be present in aqueous solution of PEG-2; the encapsulation of oxometalporphyrin cores by PEG chains in this system somewhat resembles that by protein chains in native enzymes.

As shown in Figure 2, addition of [D₈]dioxane to a solution of PEG-1 in D₂O leads to better resolved ¹⁹F NMR signals. Probably, increasing the content of dioxane or decreas-

ing the content of water in the solution renders the micelles less compact and improves the solvation of the porphyrin core. This is consistent with the increase in particle size with decreasing water content as observed by dynamic light scattering measurements (Figure 5). A related phenomenon was previously observed for a water-soluble dendrimer, which, in aqueous solution, swells progressively like dried sponges upon addition of THF.^[17]

Figure 7 shows a proposed change in the microenvironment of ruthenium porphyrin moiety in PEG-1 as the solvent changes from dioxane to dioxane–water and to water,

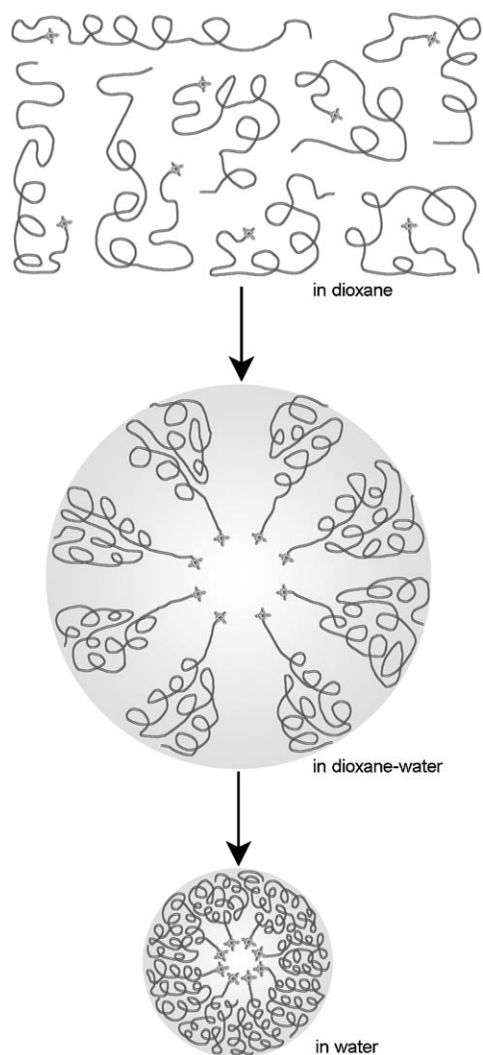


Figure 7. Schematic diagram showing proposed change in microenvironment of ruthenium porphyrin core in PEG-1 upon changing solvent from dioxane to dioxane–water and to water.

which should be applicable to the case of PEG-2 as well. We propose that, in dioxane, the PEG-supported ruthenium porphyrins exhibit a “loose” structure and are well solvated. When the solvent polarity is increased by the addition of water, formation of micellar aggregates occurs. The micelles become more compact at higher water contents, and in water, the ruthenium porphyrin cores are probably “frozen”

and “tightly” protected by the PEG chains. This might be a reason for the remarkable stability of PEG-2 in water.

A “loose” arrangement of the PEG chain is also expected in CDCl_3 , in which case there might not be significant interaction between styrene and PEG protons, accounting for the absence of NOE between styrene and PEG protons in the 2D NMR spectrum recorded in this solvent (see Figure 3). However, in D_2O , the interaction of the hydrophilic part of PEG chain with D_2O would cause the hydrophobic part of PEG and styrene molecules to form a hydrophobic region, wherein the interaction between styrene and PEG protons could be sufficiently strong to allow observation of NOE (Figure 3).

Kinetic studies of hydrocarbon oxidation by PEG-2: Inspection of the data in Table 6 reveals that attachment of **2** to PEG slightly retards the reaction of dioxoruthenium(vi) porphyrin with hydrocarbons ($k_2(\mathbf{2})/k_2(\text{PEG-2})=1.1\text{--}1.8$) in $\text{ClCH}_2\text{CH}_2\text{Cl}$ and the reactions of PEG-2 or **2** with ethylbenzene and cumene (entries 12 and 13) are much slower than those with styrenes (entries 1–7, 9, and 10). The epoxidation by PEG-2 displays a larger k_2 value for *trans*- β -methylstyrene and *trans*-stilbene than for *cis*- β -methylstyrene and *cis*-stilbene, respectively, like that by **2**. In previous studies of dioxoruthenium(vi) complexes with sterically bulky porphyrin ligands,^[13d,f] the k_2 value for the epoxidation of *trans*- β -methylstyrene or *trans*-stilbene is smaller than that for *cis*- β -methylstyrene or *cis*-stilbene; this result arises from larger steric interaction of *trans*- than *cis*-alkene with bulky porphyrin ligands. This suggests that, in organic solvent, the porphyrin core of PEG-2 has a similar steric environment to that of **2**.

Our previous work demonstrated that oxidation of styrenes $p\text{-X-C}_6\text{H}_4\text{CH=CH}_2$ ($\text{X}=\text{H, F, Cl, Me, MeO}$) with other dioxoruthenium(vi) porphyrins, such as $[\text{Ru}^{\text{VI}}(2,6\text{-Cl}_2\text{tpp})\text{O}_2]$, exhibits a linear dual-parameter Hammett correlation $\log k_{\text{rel}} = \rho_{\text{mb}}\sigma_{\text{mb}} + \rho_{\text{JJ}}\sigma_{\text{JJ}}$ (in which $k_{\text{rel}} = k_2(\text{X})/k_2(\text{H})$), with ρ_{mb} ranging from -0.58 to -0.77 and ρ_{JJ} from 1.01 to 1.67 ($|\rho_{\text{JJ}}/\rho_{\text{mb}}| = 1.63\text{--}2.17$).^[13e,f] From the data in Table 6, we obtained a similar Hammett correlation, $\log k_{\text{rel}} = -0.59\sigma_{\text{mb}} + 0.96\sigma_{\text{JJ}}$ ($R = 0.98$, $|\rho_{\text{JJ}}/\rho_{\text{mb}}| = 1.63$) for **2** and $\log k_{\text{rel}} = -0.56\sigma_{\text{mb}} + 1.20\sigma_{\text{JJ}}$ ($R = 0.99$, $|\rho_{\text{JJ}}/\rho_{\text{mb}}| = 2.07$) for PEG-2. Apparently, the oxidation of styrenes in $\text{ClCH}_2\text{CH}_2\text{Cl}$ by these dioxoruthenium(vi) porphyrins proceeds through a similar mechanism.

From the data in Table 7 it is evident that for the oxidation of styrene by PEG-2 in dioxane–water, when water content increases from 40% to 60%, the k_2 value increases gradually and reaches $(89.0 \pm 2.0) \times 10^{-3} \text{ dm}^3 \text{ mol}^{-1} \text{ s}^{-1}$, which is 11.6 times that obtained in $\text{ClCH}_2\text{CH}_2\text{Cl}$. As water content reaches 65%, the k_2 value increases to $(304.8 \pm 8.9) \times 10^{-3} \text{ dm}^3 \text{ mol}^{-1} \text{ s}^{-1}$. At a water content of 70%, k_2 increases dramatically and reaches $(479.0 \pm 39.5) \times 10^{-3} \text{ dm}^3 \text{ mol}^{-1} \text{ s}^{-1}$, which is 62 times that obtained in $\text{ClCH}_2\text{CH}_2\text{Cl}$. With further increase in water content to 80% and 90%, the k_2 value increases slightly to $(548.0 \pm 37.3) \times 10^{-3}$ and $(570.9 \pm 28.1) \times 10^{-3} \text{ dm}^3 \text{ mol}^{-1} \text{ s}^{-1}$, respectively.

The effect of water content on the reaction of PEG-2 with ethylbenzene in dioxane–water is similar to, or even larger than, that observed with styrene. When the water content increases from 40% to 60%, the k_2 value increases gradually and reaches $(15.5 \pm 0.9) \times 10^{-3} \text{ dm}^3 \text{ mol}^{-1} \text{ s}^{-1}$, which is 19 times that obtained in $\text{ClCH}_2\text{CH}_2\text{Cl}$. A faster increase of k_2 occurs at a water content of 65%, with the k_2 value reaching $(39.9 \pm 3.1) \times 10^{-3} \text{ dm}^3 \text{ mol}^{-1} \text{ s}^{-1}$. As the water content increases to 80%, the k_2 value increases to $(152.0 \pm 9.7) \times 10^{-3} \text{ dm}^3 \text{ mol}^{-1} \text{ s}^{-1}$, which is 188 times that obtained in $\text{ClCH}_2\text{CH}_2\text{Cl}$! When the water content reaches 90%, there is a slight increase of k_2 to $(161.3 \pm 14.7) \times 10^{-3} \text{ dm}^3 \text{ mol}^{-1} \text{ s}^{-1}$.

Figure 8 shows the k_2 versus water content plots for the oxidation of styrene and ethylbenzene by PEG-2 in dioxane–water. Such plots resemble the $\Delta\delta$ versus water content plot (Figure 4) and closely correlate with the particle size versus water content plot (Figure 5). For example, the most dramatic changes in k_2 , $\Delta\delta$, and micelle size all occur at a change in water content from ~60 to ~70%. Considering

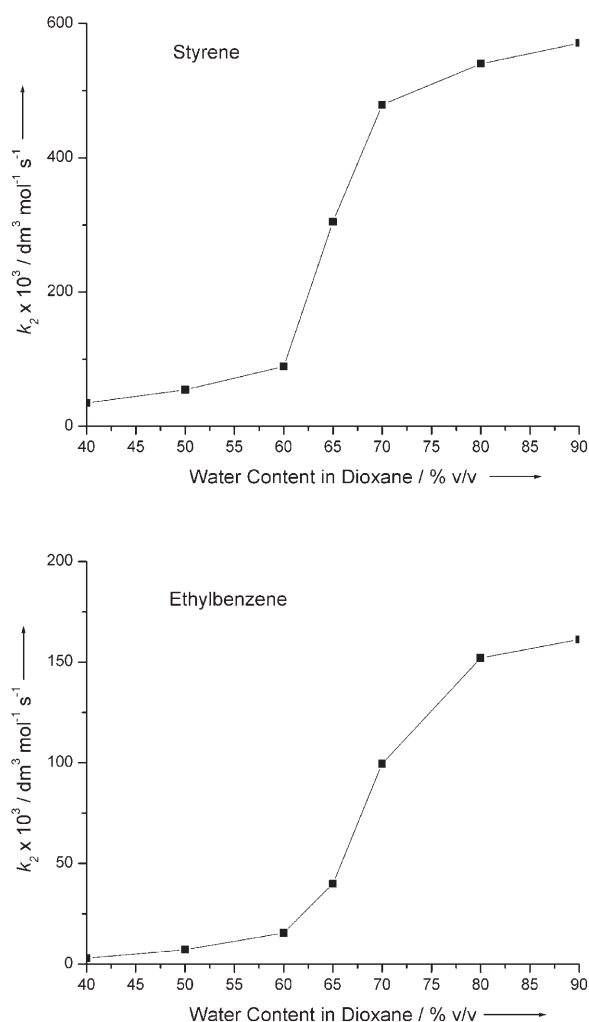


Figure 8. Variation of k_2 with different water contents for oxidation of styrene and ethylbenzene by PEG-2 in dioxane–water containing pyrazole (2% w/w) at 298 K.

the observed NOE between styrene and PEG chain in D_2O (Figure 3), the above water-induced rate acceleration is attributed to the change in interaction between the hydrocarbon substrate and PEG chain upon addition of water. Such a change in the interaction should result from hydrophobic effect, the involvement of which in some organic reactions that exhibit increased rate in water has previously been demonstrated by Breslow and co-workers.^[24a]

It can be seen that PEG plays an important role in the hydrocarbon oxidation in aqueous media, which not only prohibits the formation of μ -oxoruthenium porphyrin dimers, but could also serve as a vehicle to facilitate the dissolution of dioxoruthenium(vi) porphyrin in water and to create a micellar environment for the reactive dioxoruthenium(vi) porphyrin species.

Conclusion

Treatment of $[\text{Ru}^{\text{II}}(\text{F}_{20}\text{-tpp})(\text{CO})]$ with PEG sodium salt in DMF results in the covalent attachment of $[\text{Ru}^{\text{II}}(\text{F}_{20}\text{-tpp})(\text{CO})]$ to the PEG chains. The PEG-supported $[\text{Ru}^{\text{II}}(\text{F}_{20}\text{-tpp})(\text{CO})]$ (PEG-1) could be oxidized to PEG-supported dioxoruthenium(vi) porphyrin PEG-2 by *m*-CPBA in CH_2Cl_2 , dioxane, and water. PEG-1 exhibits high catalytic activity in 2,6- Cl_2 pyNO oxidation of cholesterol acetate and glycol as well as styrene, cyclooctene, ethylbenzene, and indane. In catalytic $\text{PhI}=\text{NTs}$ aziridination/amidation of hydrocarbons, PEG-1 exhibits an efficiency comparable to that of $[\text{Ru}^{\text{II}}(\text{F}_{20}\text{-tpp})(\text{CO})]$. PEG-1 is also an active catalyst for intramolecular amidation of sulfamate esters with $\text{PhI}(\text{OAc})_2$, representing the first efficient polymer-supported metalloporphyrin catalyst for such a C–N bond formation reaction. The catalytic properties of PEG-1 are superior to those of previously reported PEG-supported ruthenium porphyrin catalysts. Stoichiometric oxidations of hydrocarbons, such as styrene and ethylbenzene, by PEG-2 in CH_2Cl_2 gave oxidation products in up to 80% yield. Kinetic studies on the oxidation of hydrocarbons by PEG-2 in CH_2Cl_2 , benzene, and $\text{ClCH}_2\text{CH}_2\text{Cl}$ showed slightly lower reactivity than that by $[\text{Ru}^{\text{VI}}(\text{F}_{20}\text{-tpp})\text{O}_2]$. In dioxane–water mixtures containing 40–90% (v/v) water, the reactivity of PEG-2 toward oxidation of styrene and ethylbenzene increases with water content. The isolation of reactive PEG-supported dioxoruthenium(vi) porphyrin PEG-2 provides a useful model system for studying the mechanism of oxygen-atom transfer reactions involving macromolecule-supported oxometalloporphyrin intermediates.

Experimental Section

General: PEG (Aldrich, monomethylate, Mw=5000) was used as received. The alkene substrates were purified by passing through a column of activated alumina before use. 2,6- Cl_2 pyNO,^[27] $\text{PhI}=\text{NTs}$,^[28] sulfamate esters **43–46**,^[22a] and complexes **1**^[14] and **2**^[14,29] were prepared by the literature methods. All solvents were of AR grade. ^1H NMR and ^{19}F NMR spectra were measured on a Bruker DPX 300 or 400 spectrometer. Infra-

red spectra (KBr pellets) were recorded on a Bio-Rad FTS-7 FT-IR spectrometer. UV/Visible spectra were measured on a Milton Roy Spectronic 3000 diode-array spectrophotometer. Gas chromatography was performed on a Hewlett–Packard 5890 Series II gas chromatograph equipped with a flame ionization detector and a 3396 Series II integrator.

Preparation of PEG-supported carbonylthienium(III) porphyrin PEG-1: NaH (2.3 mg, 60% in oil, 0.06 mmol) was added to a solution of PEG (200 mg, 0.04 mmol) in DMF (10 mL). The mixture was stirred at room temperature for 2 h, followed by addition of a solution of **1** (112.5 mg, 0.1 mmol) in DMF (10 mL). The resulting solution was vigorously stirred at 60°C for 3 days under argon and then cooled to room temperature, poured into water, and extracted with CH₂Cl₂ (3×30 mL). The organic layer was dried with anhydrous Na₂SO₄ for 12 h. Upon removal of solvent in vacuo and subsequent addition of diethyl ether (20 mL), the precipitate was filtered quickly under argon and dried in vacuo. The crude red solid was dissolved in distilled water (2 mL) and purified by Sephadex-25 gel. The red band was collected. Removal of water under reduced pressure gave PEG-1 as a red solid. Yield: 70% (based on the amount of starting PEG); UV/Vis (CH₂Cl₂): λ_{max}=406 (Soret), 526 nm (β); IR: ν̄=1954 cm⁻¹ (CO); ¹H NMR (CDCl₃): δ=8.82 (brs, 8H), 4.78 (m, 2H; -CH₂CH₂O-por), 4.06 (m, 2H; -CH₂CH₂O-por), 3.80–3.45 (m, PEG CH₂), 3.35 ppm (s, PEG MeO); ¹⁹F NMR (CDCl₃): δ=-136.7 to -141.5 (m, 8*o*-F), -151.9 to -152.6 (m, 3*p*-F), -157.0 to -158.2 (m, 4*m*-F), -161.3 to -163.0 ppm (m, 4*m*-F).

Preparation of PEG-supported dioxoruthenium(VI) porphyrin PEG-2: Excess *m*-CPBA (40 mg) was added to a CH₂Cl₂ (5 mL) solution of PEG-1 (60 mg). The resulting solution was stirred for 3 min. When the color of the solution changed to dark purple, anhydrous diethyl ether (25 mL) was added. The precipitate was quickly collected by filtration and dried in vacuo at room temperature, affording PEG-2 as a dark brown hygroscopic solid. Yield: 80%; UV/Vis (CH₂Cl₂): λ_{max}=414 (Soret), 508 nm (β); IR: ν̄=830 cm⁻¹ (RuO₂); ¹H NMR (CDCl₃): δ=9.20 (brs, 8H), 4.76 (m, 2H; -CH₂CH₂O-por), 4.08 (m, 2H; -CH₂CH₂O-por), 3.80–3.45 (m, PEG CH₂), 3.35 ppm (s, PEG MeO); ¹⁹F NMR (CDCl₃): δ=-135.6 to -139.0 (m, 8*o*-F), -150.4 (m, 3*p*-F), -157.6 to -161.5 ppm (m, 8*m*-F).

Oxidation of hydrocarbons with 2,6-Cl₂pyNO catalyzed by PEG-1: A mixture of hydrocarbon (1 mmol), catalyst PEG-1 (1 μmol), and 2,6-Cl₂pyNO in CH₂Cl₂ (5 mL) was stirred under argon. The amount of 2,6-Cl₂pyNO and the reaction time and temperature are indicated in Tables 1 and 2. At the end of the reaction, the mixture was evaporated to dryness. The organic products in the residue were extracted with diethyl ether, and were identified by GC in the cases in which the corresponding authentic samples were available or by comparison with previously reported ¹H NMR spectral data.

Aziridination/amidation of hydrocarbons with PhI=NTs catalyzed by PEG-1: A mixture of hydrocarbon (0.75 mmol), PhI=NTs (1.5 mmol), and PEG-1 (10 μmol) in CH₂Cl₂ (5 mL) was stirred under argon at 40°C. The reaction was followed by GC. After removal of solvent under reduced pressure, dry diethyl ether (20 mL) was added to the mixture and the solution was left to stand at 0°C for 1 h. The catalyst was filtered and was washed with cold diethyl ether (5 mL×2). The filtrate and diethyl ether washing were combined. Upon removal of solvent, the residue was purified by column chromatography on silica gel using hexane/ethyl acetate (20:1) as eluent.

Intramolecular amidation of sulfamate esters with PhI(OAc)₂ catalyzed by PEG-1: CH₂Cl₂ (1.5 mL) was added through syringe into a Schlenk flask containing sulfamate ester (0.18 mmol), PhI(OAc)₂ (0.36 mmol), PEG-1 (2.4 μmol), Al₂O₃ (0.44 mmol), and molecular sieves (4 Å, 50 mg) under argon. The mixture was stirred at 40°C for 6 h, diluted with CH₂Cl₂ (5 mL) after being cooled to room temperature, and filtered through Celite. The residue on Celite was washed with CH₂Cl₂ (2×5 mL). Evaporation of the combined filtrates under reduced pressure followed by chromatography on a silica gel column with CH₂Cl₂ as eluent afforded the corresponding cyclic sulfamidate as a white solid.

Kinetic studies: A solution of PEG-2 in ClCH₂CH₂Cl or dioxane–H₂O containing pyrazole (2% w/w) was treated with at least 100-fold excess of hydrocarbon substrate at 298±0.2 K. The absorbance (*A*) of the Soret

band in the UV/Vis spectrum of the reaction mixture at different reaction time (*t*) was measured, by using standard 1.0 cm quartz cuvettes, on a Hewlett–Packard 8453 diode array spectrophotometer interfaced with an IBM-compatible PC and equipped with a Lauda RM6 circulating water bath. A nonlinear least-squares fitting of the (*A_t*–*A_i*) versus *t* data over four half-lives (*t*_{1/2}) by the equation (*A_t*–*A_i*)=(*A_t*–*A_i*)exp(–*k*_{obs}*t*) (in which *A_t* and *A_i* are the final and initial absorbance, respectively, and *A_t* is the absorbance measured at time *t*) gave the pseudo-first order rate constant *k*_{obs} of the reaction. Upon determination of the *k*_{obs} values at various concentrations of the hydrocarbon substrate, the second-order rate constant *k*₂ of the reaction was obtained from the linear least-squares fitting of the *k*_{obs} versus hydrocarbon concentration plot. No rate saturation was observed over the hydrocarbon concentrations employed in this work.

Dynamic light-scattering studies: All measurements were performed at 25°C on Zetasizer 3000HS equipped with a 633 nm He-Ne laser using back-scattering detection. The sample solutions (1 mg mL⁻¹) were filtered through 0.20 μm filters. The scattered light of a vertically polarized He-Ne laser was measured at an angle of 90.0° and was collected on an auto-correlator. The polydispersity factor of micelles, μ₂/Γ² (in which μ₂ is the second cumulant of the decay function and Γ is the average characteristic line width), was determined and listed in Table S2. The dependence of Γ on *K*² (*K*=4π*n*sin(θ/2)/λ, in which *n* is the refractive index of the solution, θ is the scattering angle, and λ is the wavelength of the incident beam) was used to determine the diffusion coefficient *D*₀ of the micellar aggregates. The hydrodynamic diameters (*d_h*) of micelles were calculated using the Stokes–Einstein relationship [Eq. (1)], in which *k_B* is the Boltzmann constant, *T* is the absolute temperature, and η₀ is the viscosity of the solvent at *T*.

$$D_0 = \frac{k_B T}{3\pi\eta_0 d_h} \quad (1)$$

Acknowledgements

This work was supported by The University of Hong Kong (University Development Fund), the Hong Kong Research Grants Council (HKU 7011/04P), and the University Grants Committee of the Hong Kong SAR of China (Area of Excellence Scheme, AoE/P-10/01).

- [1] For reviews, see: a) B. Meunier, *Chem. Rev.* **1992**, *92*, 1411; b) J. P. Collman, X. Zhang, V. J. Lee, E. S. Uffelman, J. I. Brauman, *Science* **1993**, *261*, 1404; c) D. Dolphin, T. G. Traylor, L. Y. Xie, *Acc. Chem. Res.* **1997**, *30*, 251; d) J. L. McLain, J. Lee, J. T. Groves, in *Biomimetic Oxidations Catalyzed by Transition Metal Complexes* (Ed.: B. Meunier), Imperial College Press, London, **2000**, p. 91; e) P. Müller, C. Fruit, *Chem. Rev.* **2003**, *103*, 2905; f) P. Dauban, R. H. Dodd, *Synlett* **2003**, 1571; g) P. Tagliatesta, B. Floris, P. Galloni, *J. Porphyrins Phthalocyanines* **2003**, *7*, 351; h) G. Simonneaux, P. Tagliatesta, *J. Porphyrins Phthalocyanines* **2004**, *8*, 1166; i) G. Maas, *Chem. Soc. Rev.* **2004**, *33*, 183; j) Q.-H. Xia, H.-Q. Ge, C.-P. Ye, Z.-M. Liu, K.-X. Su, *Chem. Rev.* **2005**, *105*, 1603.
- [2] For examples of insoluble polymer-supported metalloporphyrin catalysts, see: a) X.-Q. Yu, J.-S. Huang, W.-Y. Yu, C.-M. Che, *J. Am. Chem. Soc.* **2000**, *122*, 5337; b) O. Nestler, K. Severin, *Org. Lett.* **2001**, *3*, 3907; c) E. Brulé, Y. R. de Miguel, *Tetrahedron Lett.* **2002**, *43*, 8555; d) S. Tangestaninejad, M. H. Habibi, V. Mirkhani, M. Moghadam, *Molecules* **2002**, *7*, 264; e) B. G. Choi, R. Song, W. Nam, B. Jeong, *Chem. Commun.* **2005**, 2960; f) E. Burri, M. Ohm, C. Dague-net, K. Severin, *Chem. Eur. J.* **2005**, *11*, 5055.
- [3] For examples of silica material-supported metalloporphyrin catalysts, see: a) B.-Z. Zhan, X.-Y. Li, *Chem. Commun.* **1998**, 349; b) B. T. Holland, C. Walkup, A. Stein, *J. Phys. Chem. B* **1998**, *102*, 4301; c) C.-J. Liu, W.-Y. Yu, S.-G. Li, C.-M. Che, *J. Org. Chem.* **1998**, *63*, 7364; d) V. Schünemann, A. X. Trautwein, I. M. C. M. Rietjens,

- M. G. Boersma, C. Veeger, D. Mandon, R. Weiss, K. Bahl, C. Colapietro, M. Piech, R. N. Austin, *Inorg. Chem.* **1999**, *38*, 4901; e) S. Evans, J. R. Lindsay Smith, *J. Chem. Soc. Perkin Trans. 2* **2001**, 174; f) J.-L. Zhang, Y.-L. Liu, C.-M. Che, *Chem. Commun.* **2002**, 2906; g) D. E. De Vos, M. Dams, B. F. Sels, P. A. Jacobs, *Chem. Rev.* **2002**, *102*, 3615 and the references therein.
- [4] For examples of soluble polymer-supported or dendritic metalloporphyrin catalysts, see: a) P. Bhyrappa, J. K. Young, J. S. Moore, K. S. Suslick, *J. Am. Chem. Soc.* **1996**, *118*, 5708; b) M. Kimura, T. Shiba, M. Yamazaki, K. Hanabusa, H. Shirai, N. Kobayashi, *J. Am. Chem. Soc.* **2001**, *123*, 5636; c) J.-L. Zhang, H.-B. Zhou, J.-S. Huang, C.-M. Che, *Chem. Eur. J.* **2002**, *8*, 1554; d) J.-L. Zhang, C.-M. Che, *Org. Lett.* **2002**, *4*, 1911; e) C.-Y. Zhou, W.-Y. Yu, C.-M. Che, *Org. Lett.* **2002**, *4*, 3235; f) M. Benaglia, T. Danelli, G. Pozzi, *Org. Biomol. Chem.* **2003**, *1*, 454; g) C.-M. Che, J.-S. Huang, J.-L. Zhang, *C. R. Chim.* **2003**, *6*, 1105.
- [5] For reviews, see: a) D. Mansuy, *Coord. Chem. Rev.* **1993**, *125*, 129; b) Y. Murakami, J.-i. Kikuchi, Y. Hisaeda, O. Hayashida, *Chem. Rev.* **1996**, *96*, 721; c) E. Rose, A. Lecas, M. Quelquejeu, A. Kossanyi, B. Boitrel, *Coord. Chem. Rev.* **1998**, *178–180*, 1407.
- [6] a) R. Breslow, Y. Huang, X. J. Zhang, J. Yang, *Proc. Natl. Acad. Sci. USA* **1997**, *94*, 11156; b) J. Yang, R. Breslow, *Angew. Chem.* **2000**, *112*, 2804; *Angew. Chem. Int. Ed.* **2000**, *39*, 2692; c) S. Belvedere, R. Breslow, *Bioorg. Chem.* **2001**, *29*, 321; d) J. Yang, B. Gabriele, S. Belvedere, Y. Huang, R. Breslow, *J. Org. Chem.* **2002**, *67*, 5057; e) R. Breslow, Z. L. Fang, *Tetrahedron Lett.* **2002**, *43*, 5197.
- [7] a) J. T. Groves, R. Neumann, *J. Am. Chem. Soc.* **1987**, *109*, 5045; b) J. T. Groves, R. Neumann, *J. Am. Chem. Soc.* **1989**, *111*, 2900.
- [8] R. R. French, P. Holzer, M. G. Leuenberger, W.-D. Woggon, *Angew. Chem.* **2000**, *112*, 1321; *Angew. Chem. Int. Ed.* **2000**, *39*, 1267.
- [9] P. Thordarson, E. J. A. Bijsterveld, A. E. Rowan, R. J. M. Nolte, *Nature* **2003**, *424*, 915.
- [10] a) T. Sagawa, H. Ishida, K. Urabe, K. Yoshinaga, K. Ohkubo, *J. Chem. Soc. Perkin Trans. 2* **1993**, 1; b) T. Sagawa, H. Ishida, K. Urabe, K. Yoshinaga, K. Ohkubo, *J. Mol. Catal.* **1993**, *81*, L13.
- [11] M. Nango, T. Iwasaki, Y. Takeuchi, Y. Kurono, J. Tokuda, R. Oura, *Langmuir* **1998**, *14*, 3272.
- [12] Selected examples or reviews: a) C. K. Chang, M.-S. Kuo, *J. Am. Chem. Soc.* **1979**, *101*, 3413; b) D.-H. Chin, A. L. Balch, G. N. La Mar, *J. Am. Chem. Soc.* **1980**, *102*, 1446; c) J. T. Groves, R. C. Haushalter, M. Nakamura, T. E. Nemo, B. J. Evans, *J. Am. Chem. Soc.* **1981**, *103*, 2884; d) A. L. Balch, Y.-W. Chan, R.-J. Cheng, G. N. La Mar, L. Latos-Grazynski, M. W. Renner, *J. Am. Chem. Soc.* **1984**, *106*, 7779; e) J. T. Groves, M. K. Stern, *J. Am. Chem. Soc.* **1988**, *110*, 8628; f) J. M. Garrison, D. Ostović, T. C. Bruice, *J. Am. Chem. Soc.* **1989**, *111*, 4960; g) K. Yamaguchi, Y. Watanabe, I. Morishima, *J. Chem. Soc. Chem. Commun.* **1992**, 1721; h) D. Ostovic, G.-X. He, T. C. Bruice, in *Metalloporphyrins in Catalytic Oxidations* (Ed.: R. A. Sheldon), Marcel Dekker, New York, **1994**, Chapter 2, p. 29; i) J. T. Groves, J. Lee, S. S. Marla, *J. Am. Chem. Soc.* **1997**, *119*, 6269; j) M. Schappacher, J. L. Putaux, C. Lefebvre, A. Deffieux, *J. Am. Chem. Soc.* **2005**, *127*, 2990.
- [13] a) J. T. Groves, R. Quinn, *Inorg. Chem.* **1984**, *23*, 3844; b) W.-H. Leung, C.-M. Che, *J. Am. Chem. Soc.* **1989**, *111*, 8812; c) P. Le Maux, H. Bahri, G. Simonneaux, *J. Chem. Soc. Chem. Commun.* **1994**, 1287; d) C.-J. Liu, W.-Y. Yu, S.-M. Peng, T. C. W. Mak, C.-M. Che, *J. Chem. Soc. Dalton Trans.* **1998**, 1805; e) C.-J. Liu, W.-Y. Yu, C.-M. Che, C.-H. Yeung, *J. Org. Chem.* **1999**, *64*, 7365; f) R. Zhang, W.-Y. Yu, H.-Z. Sun, W.-S. Liu, C.-M. Che, *Chem. Eur. J.* **2002**, *8*, 2495.
- [14] J. T. Groves, M. Bonchio, T. Carofiglio, K. Shalyaev, *J. Am. Chem. Soc.* **1996**, *118*, 8961.
- [15] P. Battioni, O. Brigaud, H. Desvaux, D. Mansuy, T. G. Traylor, *Tetrahedron Lett.* **1991**, 32, 2893.
- [16] a) J. Kriz, B. Masar, H. Pospisil, J. Plestil, Z. Tuzar, M. A. Kiselev, *Macromolecules* **1996**, *29*, 7853; b) M. Mizusaki, Y. Morishima, F. M. Winnik, *Macromolecules* **1999**, *32*, 4317.
- [17] J. Leclaire, Y. Coppel, A.-M. Caminade, J.-P. Majoral, *J. Am. Chem. Soc.* **2004**, *126*, 2304.
- [18] R. C. Larock, *Comprehensive Organic Transformations: A Guide to Functional Group Preparations*, VCH, New York, **1989**, p. 505.
- [19] R. L. Halcomb, S. J. Danishefsky, *J. Am. Chem. Soc.* **1989**, *111*, 6661.
- [20] Selected examples: a) S.-M. Au, J.-S. Huang, W.-Y. Yu, W.-H. Fung, C.-M. Che, *J. Am. Chem. Soc.* **1999**, *121*, 9120; b) X.-Q. Yu, J.-S. Huang, X.-G. Zhou, C.-M. Che, *Org. Lett.* **2000**, *2*, 2233; c) X.-G. Zhou, X.-Q. Yu, J.-S. Huang, C.-M. Che, *Chem. Commun.* **1999**, 2377; d) J.-L. Liang, J.-S. Huang, X.-Q. Yu, N. Zhu, C.-M. Che, *Chem. Eur. J.* **2002**, *8*, 1563; e) J.-L. Liang, S.-X. Yuan, J.-S. Huang, W.-Y. Yu, C.-M. Che, *Angew. Chem.* **2002**, *114*, 3615; *Angew. Chem. Int. Ed.* **2002**, *41*, 3465.
- [21] Selected examples: a) R. Breslow, S. H. Gellman, *J. Chem. Soc. Chem. Commun.* **1982**, 1400; b) R. Breslow, S. H. Gellman, *J. Am. Chem. Soc.* **1983**, *105*, 6728; c) J. P. Mahy, G. Bedi, P. Battioni, D. Mansuy, *Tetrahedron Lett.* **1988**, *29*, 1927; d) J. Yang, R. Weinberg, R. Breslow, *Chem. Commun.* **2000**, 531.
- [22] a) C. G. Espino, P. M. Wehn, J. Chow, J. Du Bois, *J. Am. Chem. Soc.* **2001**, *123*, 6935; b) P. M. Wehn, J. Du Bois, *J. Am. Chem. Soc.* **2002**, *124*, 12950; c) P. M. Wehn, J. Lee, J. Du Bois, *Org. Lett.* **2003**, *5*, 4823; d) A. Hinman, J. Du Bois, *J. Am. Chem. Soc.* **2003**, *125*, 11510.
- [23] a) J. M. Harris, *Poly(ethylene glycol) Chemistry: Biotechnical and Biomedical Applications*, Plenum, New York, **1992**; b) *Metal Complexes and Metals in Macromolecules: Synthesis, Structure and Properties*, (Eds.: D. Wöhrle, A. D. Pomogailo), Wiley-VCH, Weinheim, **2003**; c) *Polymeric Materials in Organic Synthesis and Catalysis* (Ed.: M. R. Buchmeiser), Wiley-VCH, Weinheim, **2003**.
- [24] a) R. Breslow, *Acc. Chem. Res.* **1991**, *24*, 159; b) X.-K. Jiang, Y.-Z. Hui, Z.-X. Fei, *J. Am. Chem. Soc.* **1987**, *109*, 5862; c) W.-Q. Fan, X.-K. Jiang, *J. Am. Chem. Soc.* **1985**, *107*, 7680.
- [25] a) K. Persson, G. Wang, G. Olofsson, *J. Chem. Soc. Faraday Trans.* **1994**, *90*, 3555; b) H. Zhang, J. Pan, T. E. Hogen-Esch, *Macromolecules* **1998**, *31*, 2815; c) M. Valentini, A. Vaccaro, A. Rehor, A. Napoli, J. A. Hubbell, N. Tirelli, *J. Am. Chem. Soc.* **2004**, *126*, 2142.
- [26] a) C.-M. Che, J.-L. Zhang, L.-R. Lin, *Chem. Commun.* **2002**, 2556; b) N. J. Turro, P. L. Kuo, *Langmuir* **1986**, *2*, 438; c) A. Pendri, A. Martinez, J. Xia, R. G. L. Shorr, R. B. Greenwald, *Bioconjugate Chem.* **1995**, *6*, 596.
- [27] R. J. Rousseau, R. K. Robins, *J. Heterocycl. Chem.* **1965**, *2*, 196.
- [28] Y. Yamada, T. Yamamoto, M. Okawara, *Chem. Lett.* **1975**, 361.
- [29] C.-M. Che, J.-L. Zhang, R. Zhang, J.-S. Huang, T.-S. Lai, W.-M. Tsui, X.-G. Zhou, Z.-Y. Zhou, N. Zhu, C. K. Chang, *Chem. Eur. J.* **2005**, *11*, 7040.

Received: December 3, 2005

Published online: February 21, 2006